WIDTH IR LUMINEScENCE OF PRIME CENTER OF TWO-VALENT MEDIUM IN PEROVSKIT $LaAlO_3$

© 2025 A. N. Romanov[a,*], E. V. Haula[a], A. A. Kapustin[a], D. G. Filatova[b], I. A. Rodin[b], A. M. Kuli-zade[b], V. N. Korchak[a]

[a]*N.N. Semenov Federal Research Center for Chemical Physics of the Russian Academy of Sciences, , Moscow, Russia*

[b]*Lomonosov Moscow State University, Moscow, Russia*

**e-mail: alexey.romanov@list.ru*

Received September 04, 2024
Revised December 24, 2024
Accepted December 24, 2024

Abstract. In samples of $LaAlO_3$ perovskites doped with copper, broadband photoluminescence in the near infrared range was detected. Its source, apparently, is an optically active center formed at heterovalent substitution of Al^{3+}cation for Cu^{2+}. Additional introduction of tetravalent cations Sn^{4+}, Zr^{4+} and Hf^{4+} provides charge compensation of heterovalent substitution, which leads to an increase in the photoluminescence intensity of the corresponding doped materials.

Keywords: *photoluminescence, perovskite, $LaAlO_3$, divalent copper, impurity center*

DOI: 10.31857/S0002337X250303e4

INTRODUCTION

Optically active centers based on impurity Cu^{2+} ions can become the basis of promising materials for quantum electronics and photonics, but the photoluminescence (**PL**) of the divalent copper cation $Cu^{2+}$is currently insufficiently

studied. The electronic configuration of this ion (d^9) is the "hole equivalent" of the simplest configuration involving a *d* electron: d^1. But while the FL for d^1-cations ($Ti^{(3+)}$, $V^{(4+)}$)) is well known [1], there are few reports of FL observed for optically active Cu^{2+}centers. Near-infrared (**NIR**) FL has been observed previously on impurity $Cu^{(2+)}$ center in copper-doped crystalline phases of ZnS, CdS and ZnO [2-5] ($Cu^{(2+)}$ in tetrahedral coordination), in Egyptian Blue pigment and similar phases [6-8] ($Cu^{(2+)}$ in plano-square coordination), as well as in copper-doped phases $YGaO_3$, $YInO_{(3)}$, $GdInO_{(3)[9]}$] ($Cu^{(2+)}$ in trigonal-bipyramidal coordination). FL of octahedrally coordinated $Cu^{2+}$was observed for perovskite $KZnF_3$and K_2phase of ZnF_4at cryogenic temperatures (<20K) [10-12]. Rather unexpectedly, NIR-FL of Cu^{2+}impurity centers was recently detected at room temperature in the corundum lattice (α-$Al_{(^2_)\ O3}$) [13, 14]. This fact is of considerable interest, since it was previously thought that the FL of Cu^{2+}cation in octahedral coordination is hardly possible (especially at T~ 300 K), since the presence of the Jahn-Teller effect in the ground electronic state $^{(2)}E_g$of $Cu^{(2+)}$ion leads to a significant distortion of the initial geometry of the impurity center and strong electron-phonon coupling at the optical transition ($_2{}^{)}T_{(2)\ (g)}\rightarrow{}_(2_{)\ E(g)}$. This, in turn, determines a high probability of radiation-free relaxation of the excited state $^{(2)}T_{(2)\ (g)}$. Nevertheless, the existence of intense NIR-FL in copper-doped corundum proves that, even in spite of the existence of strong electron-phonon coupling leading to a significant broadening of the FL spectrum, the radiation-free decay channel of the excited state cannot completely extinguish the FL. Apparently, the decrease in the rate of Cu^{2+}radiation-free

relaxation in corundum is due to a number of factors, one of which is the large value of the crystal field in the cationic positions of α-$Al_{(^{2})\,O3}$, which leads to an increase in the energy of the excited state $^{(2)}T_1$relative to the ground state ^2E and an increase in the potential barrier of the excited state deactivation process.

The large width of the NIR-FL spectrum of impurity Cu^{2+}centers in corundum may be of practical interest, since such materials are in demand as the active medium of broadband optical amplifiers and oscillators. Therefore, it is reasonable to search for other crystalline phases in which the Cu^{2+}ion also demonstrates broadband FL. It is obvious that the most promising matrices will be those in which the Cu^{2+}ion is located under strong crystal field conditions. The perovskite $LaAlO_3$satisfies this condition, since it was shown earlier by comparing the spectral characteristics of the Cr^{3+}ion that the crystalline field in this oxide is even slightly stronger than in α-$Al_{(2)\,O(3)}$ [15]. The significant magnitude of the crystal field in the aluminum cationic position of the $LaAlO_3$lattice is also indicated by a recent study of the luminescence of impurity Ni^{2+} ions in this crystal [16]. $LaAlO_3$is a well-studied technological material, which is available in the form of large-sized single crystals, it is widely used as a substrate for the preparation of thin films of various functional materials [17, 18].

In the present work, we present for the first time the observation and study of broadband NIR-FL of an octahedrally coordinated impurity ion $Cu^{(2+)}$in the crystalline matrix $LaAlO_3$.

EXPERIMENTAL PART

Samples of perovskite $LaAlO_3$, doped with $Cu^{(2+)}$and co-doped with four-charged ions $M^{(4+)}$ (M = Ti, Ge, Zr, Hf, Sn), were prepared by coprecipitation of hydroxides of Al, La, and Cu. The coprecipitation was carried out by adding excess aqueous ammonia to a solution containing lanthanum, aluminum and copper nitrates in appropriate amounts. The resulting suspension of coprecipitated hydroxides without filtration was gently heated in a wide glass-carbon crucible until evaporation of the solution and decomposition of ammonium nitrate formed during coprecipitation (~ 400°C). The solid residue was then heated in a porcelain crucible to 900°C, extracted from the furnace, grinded in a mortar with a calculated amount of the coalescing element oxide (TiO_2, $GeO_{(2)}$, $ZrO_{(2)}$, $HfO_{(2)}$, $SnO_{(2)}$)), and subjected to final heat treatment at 1500°C for 2 h. The amount of copper and the coalescing element ($TiO_{(2)}$, $GeO_{(2)}$, ZrO_2, HfO_2, $SnO_{(2)}$)) was determined. The amount of Cu and the salt-enhancing element in the initial charge corresponded to the atomic ratios $Cu^{2+}/Al^{(3+)}$= 0.005 and $M^{4+}/Al^{(3+)}$) = 0.01.

The phase composition and lattice parameters of the obtained samples were determined by powder diffractometry using Rigaku Smartlab SE (CuK_α-radiation, λ = 1.54056 Å).

FL spectra in the NIR range were recorded using an SDH-IV spectrometer (Solar LS) equipped with a linear InGaAs sensor G9212-512 (Hamamatsu). A semiconductor laser module with an emission wavelength of 820 nm was used for FL excitation. The obtained spectra were corrected taking into account the spectral sensitivity curves of the photodetector.

The FL excitation spectra were recorded using a setup consisting of an HLX 64640 Xenophot 150W halogen lamp, an IR cutoff water filter, a LOMO MDR-206 monochromator, an SR530 optical interrupter (Stanford Instruments), a focusing system, and an InGaAs photodetector (produced by Polyus). The signal from the photodetector was fed to an SR830 synchronous amplifier phased with the SR530 interrupter. The output from the amplifier through ADC was registered on the PC. The necessary FL registration bandwidth was provided by a set of light filters (IKS-7, interference light filters Thorlabs, Edmund Optics).

RESULTS AND DISCUSSION

Figure 1 shows overview diffractograms of $LaAlO_3$samples doped with $Cu^{(2+)}$ ions and co-doped with various tetravalent cations.

The main phase in all samples (except for the solvated Cu and Ti) is the pseudo-cubic (rhombohedral) phase $LaAlO_3$, which can be removed from the cubic lattice of perovskite by imposing a small rhombohedral distortion with symmetry reduction [19]. This distortion leads only to a slight splitting of the reflexes (not noticeable in the overview diffractograms, Fig. 1) characteristic of cubic perovskite. When Cu and Ti are solvated, no splitting of the reflexes occurs, indicating that the cubic perovskite lattice is stabilized in this sample (Fig. 2). Comparatively wide reflections indicate a small area of coherent X-ray scattering. This is apparently due to the strong defectivity of the crystal lattice of this perovskite.

Broadband IR-FL was observed in all the samples studied (Fig. 3).

The NIR-FL spectra are almost identical, from which it can be concluded that there is a single type of photoluminescent center present in all samples. In Fig. 4 also shows the combined FL and FL excitation spectra for one of the obtained samples ($Cu^{2+}$and Zr^{4}coalloyed^{+})

These spectra are generally similar to those previously obtained for copper-doped corundum [13], although slightly shifted to the shorter wavelength region, apparently due to the stronger crystal field in $LaAlO_3$.

From Fig. 3 shows that the NIR-FL intensity varies greatly depending on the presence and nature of the co-doping four-charged cation. At the same time, the greatest enhancement of the FL intensity compared to the sample doped only with $Cu^{2+}$is observed when co-doped with relatively large cations: $Sn^{(4+)}$(ionic radius for EC = 6 R = 0.69 Å), $Zr^{(4+)}$(R = 0.72 Å), $Hf^{(4+)}$(R = 0.71 Å). In contrast, co-doping with a small Ge^{4+}cation (R = 0.53 Å) leads to a decrease in the FL intensity compared to the sample doped with Cu^{2+}alone . The sample co-doped with $Cu^{2+}$and a medium-sized $Ti^{(4+)}$ ion (R = 0.605 Å), also shows very weak FL, but this seems to be a consequence of the strong lattice defectivity of this sample and the difference of its lattice type from all other samples.

The revealed pattern of Cu^{2+}FL enhancement in $LaAlO_3$upon co-doping with different four-charged cations differs from that obtained earlier for $Cu^{(2+)}$-$_{doped}$corundum (α-$Al_{(}^{2}{}_{)}O3$) [13]. In this case, samples co-doped with $Ti^{4+}$and Ge^{4+}, exhibited more intense FL than those containing $Zr^{(4+)}$and Hf^{4+}. It also differs from the sequence (in order of increasing FL intensity) of the solvating cations obtained

in a recent study of the FL of impurity $Ni^{(2+)}$ion in $LaAlO_3$[16]: $Sn^{4+} > Hf^{(4+)} = Ti^{4+} > Zr^{(4+)} >$ without solvation.

Let us try to understand the reason for the different influence of the solvating cations in our case. Four-charged cations $M^{4+}$are introduced into the crystal lattice of the matrix to provide charge compensation for heterovalent substitution of $Al^{3+} \rightarrow Cu^{2+}$. Without $M^{(4+)}$doping, a significant fraction of Cu enters the lattice as Cu^{3+}. This was shown in the case of copper-doped corundum [13] and seems to be true also for perovskite $LaAlO_3$. The presence of Cu^{3+}in copper-containing $LaAlO_3$perovskites is evidenced, in particular, by their reddish-purple coloration, characteristic of $Cu(3+)$ ions. This coloration is noticeably weaker in sol-doped samples, since, with the possibility of charge compensation, copper enters the lattice predominantly in the form of Cu^{2+}cations rather than $Cu(^{3+})$.

In the corundum matrix, the most intense FL was observed in samples coalloyed with relatively small cations, $Ge^{4+}$and Ti^{4+}, because they more easily substitute Al^{3+} ions. In $LaAlO_(^3)$, in contrast, the FL is more intense in samples coalloyed only with large cations $Hf^{(4+)}$, $Zr^{(4+)}$, $Sn^{(4+)}$. This suggests that for the formation of the luminescent impurity center Cu^{2+}in $LaAlO_{(3),}$charge compensation must occur by substitution of the large cation $La^{(3+)}$rather than the small $Al^{3+}$by the coalloying ion $M^{(4+)}$. In this connection, it is interesting to note that it has recently been demonstrated how similar solvation of $LaAlO_3$by thorium dioxide with substitution of $La(^{3+)\ with} \rightarrow Th^{(4+}{}_)$(due to the large ionic radius of $Th^{(4+}{}_)$only such substitution is possible in perovskite $LaAlO_(^3)$) significantly improves the FL

parameters of $Nd^{3+}$by reducing the number of defect centers in the form of cation vacancies [20, 21]. This mechanism of PL intensity enhancement is also possible in our samples.

Additional information on the formation of Cu^{2+}impurity centers in the $LaAlO_3$matrix is provided by the data obtained from X-ray diffractograms (Fig. 5)on the change in unit cell size during copper doping and co-doping with various M^{4+}cations.

It can be seen that the unit cell size of $LaAlO_3$increases slightly when doped only with copper, apparently due to the substitution of $Al^{(3+)}$by larger cations $Cu^{3+}$and Cu^{2+}. The cell size also increases when $LaAlO_3$is doped with Zr, Sn, and Ge oxides. Simultaneous doping of $LaAlO_3$with copper and zirconium, as well as with copper and tin leads to a strong increase in the size of the crystal lattice, so that the size increment turns out to be larger than could be expected from the sum of the increments due to doping with copper or a co-doping element only. In this case, the excess increment appears to be due to the preferential substitution of $Al^{3+}$for the bulk Cu^{2+}cation (rather than the relatively small $Cu^{3+)}$, since the introduction of $Sn^{4+}$and Zr^{4+} ions into the crystal lattice can provide charge compensation for such substitution. The increase in the amount of impurity Cu^{2+} ions leads to the enhanced PL of the corresponding sol-doped samples compared to $LaAlO_3$doped only with copper.

In contrast, the crystal cell size is slightly reduced upon co-doping with germanium and copper compared to doping with germanium alone, indicating that

the additional introduction of Ge^{4+}does not promote the formation of $Cu^{(2+)}$impurity centers in $LaAlO_3$. In agreement with this finding, a decrease in the PL intensity of the sample co-doped with Ge and Cu compared to the sample doped with copper alone is observed.

CONCLUSION

Impurity Cu^{2+} ions in the $LaAlO_3$perovskite lattice exhibit broadband NIR-FL. The appearance of this FL is promoted by the large value of the crystal field on the impurity ion in the $LaAlO_3$matrix, demonstrated earlier for impurity cations $Cr^{3+}$and Ni^{2+}. The intensity of the Cu^{2+}FL increases with the additional introduction into the $LaAlO_3$lattice of some four-charged cations that act as charge compensators. The greatest PL enhancement was observed upon introduction of relatively bulk cations Sn^{4+}, $Zr^{(4+)}$, Hf^{4+}, rather than compact $Ti^{(4+)}$and Ge^{4+}. This seems to indicate that the charge compensator must replace the $La^{(3+)}$cation to form the FL center.

It is also noted that the introduction of $Ti^{(4+)}$cation as a charge compensator in $LaAlO_{(3)}$leads to the stabilization at room temperature of the high-temperature cubic modification $Pm\bar{3}m$ instead of the usual low-temperature trigonal one $R\bar{3}c$. The presence of broadband PL in $Cu^{(2+)}$:$LaAlO_3$along with the previously studied PL of $Cu_{(}^{2+)}$in $Al_{(}^{2})_{O3}$testifies to the correctness of our chosen approach to search for matrices for PL of octahedrally-coordinated impurity Cu^{2+}among crystals providing the strongest possible crystal field on the impurity ions.

FUNDING

This work was supported by the Russian Science Foundation (grant No. 23-23-00160).

CONFLICT OF INTERESTS

The authors declare that they have no conflict of interest.

FIGURE CAPTIONS

Fig. 1. Overview diffractograms of different $LaAlO_3$samples: unalloyed, copper-doped, and also coalloyed with copper and different elements (indication of the reflections is given in hexagonal system; due to close proximity many reflections are not visually resolved).

Fig. 2. Details of diffractograms of different $LaAlO_3$samples: unalloyed, Cu-doped, and also coalloyed with Cu and different elements in the region 41.2° (for all samples, except for Cu, Ti co-doped, we can see a complex structure formed by the convolution of two peaks from adjacent reflexes (202, 006) with a hardware profile formed by superposition of two reflexes - $K_{(\alpha)\,(1)}$and $K_{(\alpha)\,(2)}$; in the Cu, Ti co-doped sample there is only one split cubic perovskite reflex).

Fig. 3. PL spectra of $LaAlO_3$, doped with $Cu^{2+}$and co-doped with different tetravalent ions (the height of the spectrum corresponds to the relative PL intensity of each sample; excitation wavelength λ_{ex}= 820 nm).

Fig. 4. PL and FL excitation spectra of perovskite $LaAlO_3$, co-doped with $Cu^{(2+)}$and Zr^{4+}.

Fig. 5. Variation of crystal lattice parameters of perovskite $LaAlO_{(3)}$ (hexagonal system) when it is doped with copper, four-charged ions $M^{(4+)}$ (M = Zr, Sn, Ge), and also when it is co-doped with copper and these elements.

REFERENCES

1. *Moncorge R.* Laser Materials Based on Transition Metal Ions // Opt. Mater. 2017. V. 63. P. 105-117.

https://doi.org/10.1016/j.optmat.2016.05.060

2. *Meijer G.* Infrared Fluorescence of Copper-Activated Zinc Sulphide Phosphors // J. Phys. Phys. Chem. Solids. 1958. V. 7. № 2-3. P. 153-158.

https://doi.org/10.1016/0022-3697(58)90256-7

3. *Broser I., Maier H., Schulz H-J.* Fine Structure of the Infrared Absorption and Emission Spectra of Cu^{2+}in ZnS and CdS Crystals // Phys. Rev. A. 1965. V. 140. № 6. P. A2135-A2138.

https://doi.org/10.1103/PhysRev.140.A2135

4. *BroserI.Hoffmann A., Heitz R.*, Thurian P. Zeeman and Piezospectroscopy of the Cu^{2+}Center in CdS // J. Lumin. Lumin. 1991. V. 48-49. P. 693-697.

https://doi.org/10.1016/0022-2313(91)90221-G

5. *Kimpel B.M., Schulz H-J.* Infrared Luminescence of ZnO:$Cu^{(2+)(d9)}$) // Phys. Rev. B. 1991. V. 43. № 12-15. P. 9938-9940.

https://doi.org/10.1103/PhysRevB.43.9938

6. *Pozza G., Ajo D., Chiari G. et al.* Photoluminescence of the Inorganic Pigments Egyptian Blue, Han Blue and Han Purple // J. Cult. Cult. Heritage. 2000. V. 1. № 4. P. 393-398.

https://doi.org/10.1016/S1296-2074(00)01095-5

7. *Accorsi G., Verri G., Bolognesi M. et al.* The Exceptional Near-Infrared Luminescence Properties of Cuprorivaite (Egyptian Blue) // Chem. Commun. 2009. V. 23. P. 3392-3394.

https://doi.org/10.1039/B902563D

8. *Li Y.-J., Ye S., Wang C.-H. et al.* Temperature-Dependent Near-Infrared Emission of Highly Concentrated Cu^{2+}in $CaCuSi_{(4)}O_{10}$Phosphor // J. Mater. Mater. Chem. C. 2014. V. 2. № 48. P. 10395-10402.

https://doi.org/10.1039/C4TC01966K

9. *Romanov A.N., Haula E.V., Shashkin D.P., Korchak V.N.*. Broadband Near-IR Photoluminescence of Trigonal-bipyramidal Coordinated $Cu^{(2+)}$Impurity Center in $YGaO_3$, $YInO_3$and $GdInO_3$Hexagonal Phases // J. Lumin. Lumin. 2020. V. 228(2A). P. 117652.

https://doi.org/10.1016/j.jlumin.2020.117652

10. *Dubicki L., Krausz E., Riley M.* The First d-d Fluorescence of a Six-Coordinate Copper(II) Ion // J. Am. Am. Chem. Soc. 1989. V. 111. № 9. P. 3452-3454.

https://doi.org/10.1021/ja00191a065

11. *Dubicki L., Krausz E., Riley M.* Structured d-d Fluorescence from $CuF_{(6)}$ $^{4-}$ Doped in Cubic and Tetragonal Perovskites // Chem. Phys. Lett. 1989. V. 157. № 4. P. 315-320.

https://doi.org/10.1016/0009-2614(89)87254-9

12. *Dubicki L., Riley M., Krausz E.* Electronic Structure of the Copper (II) Ion Doped in Cubic $KZnF_3$// J. Chem. Chem. Phys. 1994. V. 101. № 3. P. 1930-1938.

https://doi.org/10.1063/1.467703

13. *Romanov A.N., Haula E.V., Kapustin A.A., Kostyukov A.A., Egorov A.E., Kuzmin V.A., Korchak V.N.*. Broadband Near Infrared Photoluminescence of Cu^{2+}-doped Corundum (α-Al_2O_3) // J. Am. Am. Ceram. Soc. 2024. V. 107. № 2. P. 979-983.

https://doi.org/10.1111/jace.19485

14. *Romanov A.N., Haula E.V., Kapustin A.A., Kuli-zadeh A.M., Korchak V.N.* Influence of salt-loading ions on IR photoluminescence of impurity Cu^{2+}centers in corundum (α-Al_2O_3) // Inorganic Materials. 2023. Т. 59. № 11. С. 1303-1308.

https://doi.org/10.31857/S0002337X23110118

15. *Adachi S.* Review-Photoluminescence Properties of Cr^{3+}-Activated Oxide Phosphors // ECS J. SolidState Sci. Technol. 2021. V. 10. P. 026001.

https://doi.org/10.1149/2162-8777/abdc01

16. *Ueda J., Minowa T., Xu J., Tanaka S., Nakanishi T., Takeda T., Tanabe S.* Highly Thermal Stable Broadband Near-Infrared Luminescence in Ni^{2+}-Doped $LaAlO_3$with Charge Compensator // ACS Appl. Opt. Opt. Mater. 2023. V. 1. № 6. P. 1128-1137.

https://doi.org/10.1021/acsaom.3c00041

17. *Tomashpolskiy Yu.Ya., Sadovskaya N.V., Rybakova L.F., Kholopova S.Yu., Borisov Yu.V.* Nanostructural features of phase formation CeO_2/$LaAlO_3$and $CeO_{(2)}$/(Ni-W) obtained by deposition from organometallic solutions // Organometallic Materials. 2011. T. 47. № 12. C. 1497-1501.

18. *Tomashpolsky Yu.Ya., Rybakova L.F., Sadovskaya N.V., Kholopova S.Yu., Borisov Yu.V.* Nanostructural features of phase formation in $YBa_2Cu_{(3)\ O7}$/$LaAlO_{(3)}$and $YBa_{(2)}Cu_{(3)\ O7}$/$CeO_{(2)\ /}$(Ni-W) obtained by deposition from organometallic solutions // Organometallic Materials 2012. T. 48. № 1. C. 51-56.

19. *Howard C.J., Kennedy B.J., Chakoumakos B.C.* Neutron powder diffraction study of rhombohedral rare-earth aluminates and the rhombohedral to cubic phase transition // J. Phys. Phys.: Condens. Matter. 2000. V. 12. P. 349-365.

https://doi.org/10.1088/0953-8984/12/4/301

20. *Huang S., Li S., Gong Q., Fang Q., Xu M., Tao S., Zhao C., Hang Y.* Optical properties of Nd,Th:$LaAlO_3$demonstrates its potential in high-energy pulsed laser // Opt. Laser Technol. 2022. V. 156. P. 108495.

https://doi.org/10.1016/j.optlastec.2022.108495

21. *Chang Y.-C., Hou D.-S., Yu Y.-D., Xie S.-S., Zhou T.* Color Center and Domain Structure in the Single Crystals of $LaAlO_3$// J. Cryst. Cryst. Growth. 1993. V. 129. № 1-2. P. 362-364.

https://doi.org/10.1016/0022-0248(93)90466-A

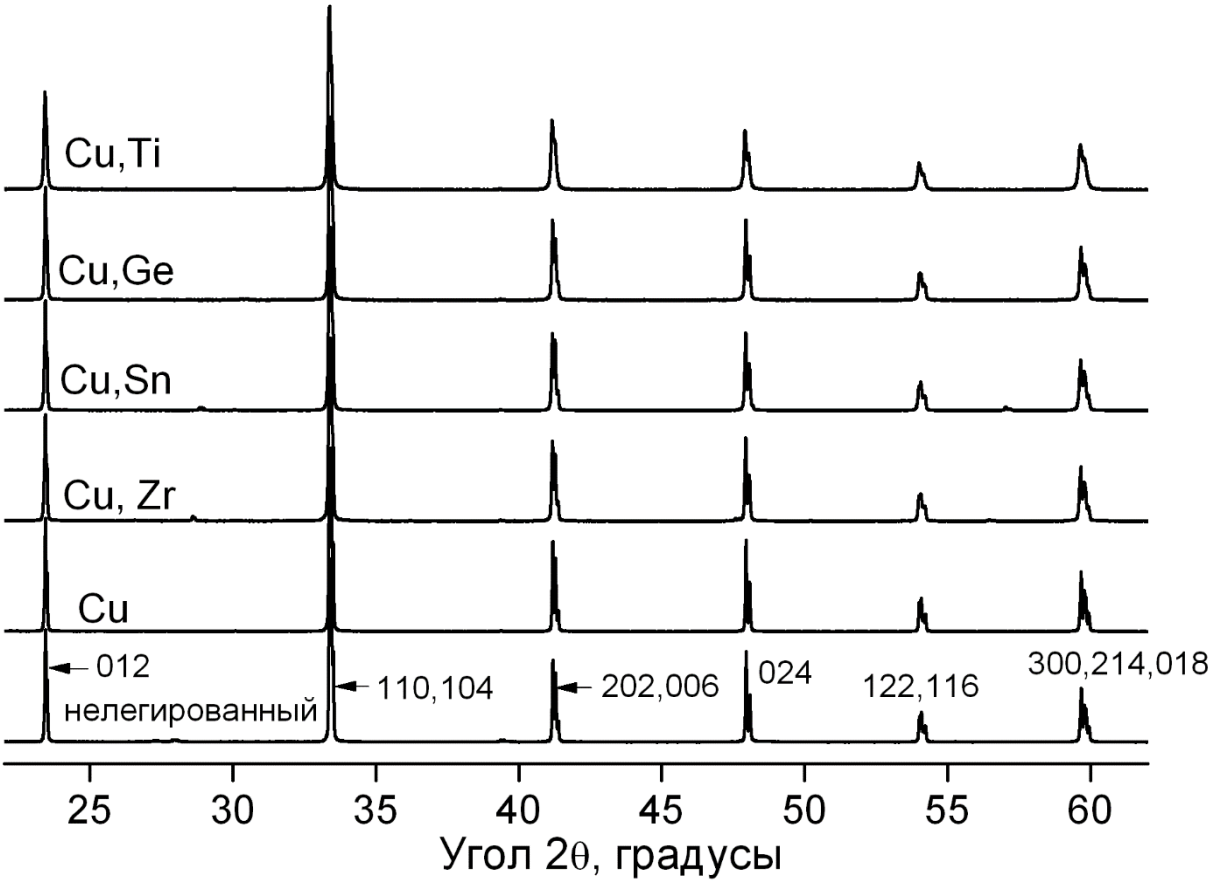
Cu,Ti
Cu,Ge
Cu,Sn
Cu, Zr
Cu
012
нелегированный
110,104
202,006
024
122,116
300,214,018
25
30
35
40
45
50
55
60
Угол 2θ, градусы

Fig. 1

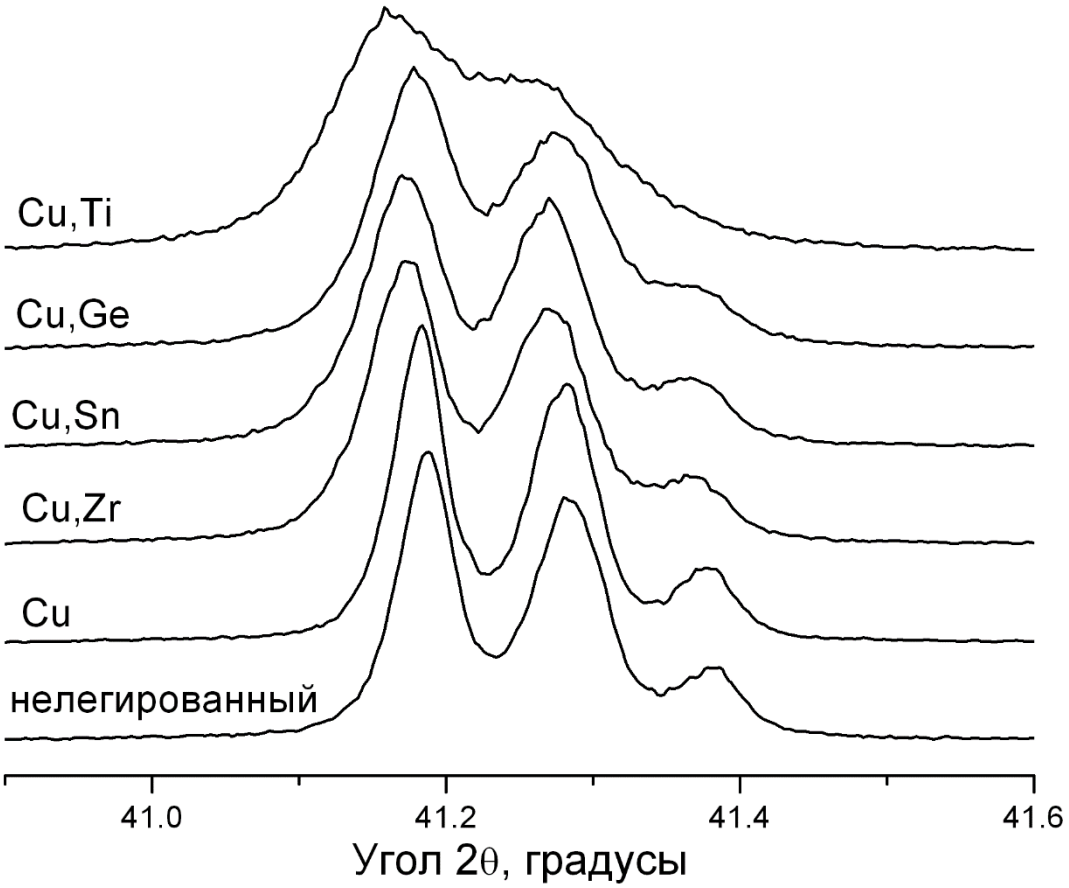
Cu,Ti
Cu,Ge
Cu,Sn
Cu,Zr
Cu
нелегированный
41.0
41.2
41.4
41.6
Угол 2θ, градусы

Fig. 2

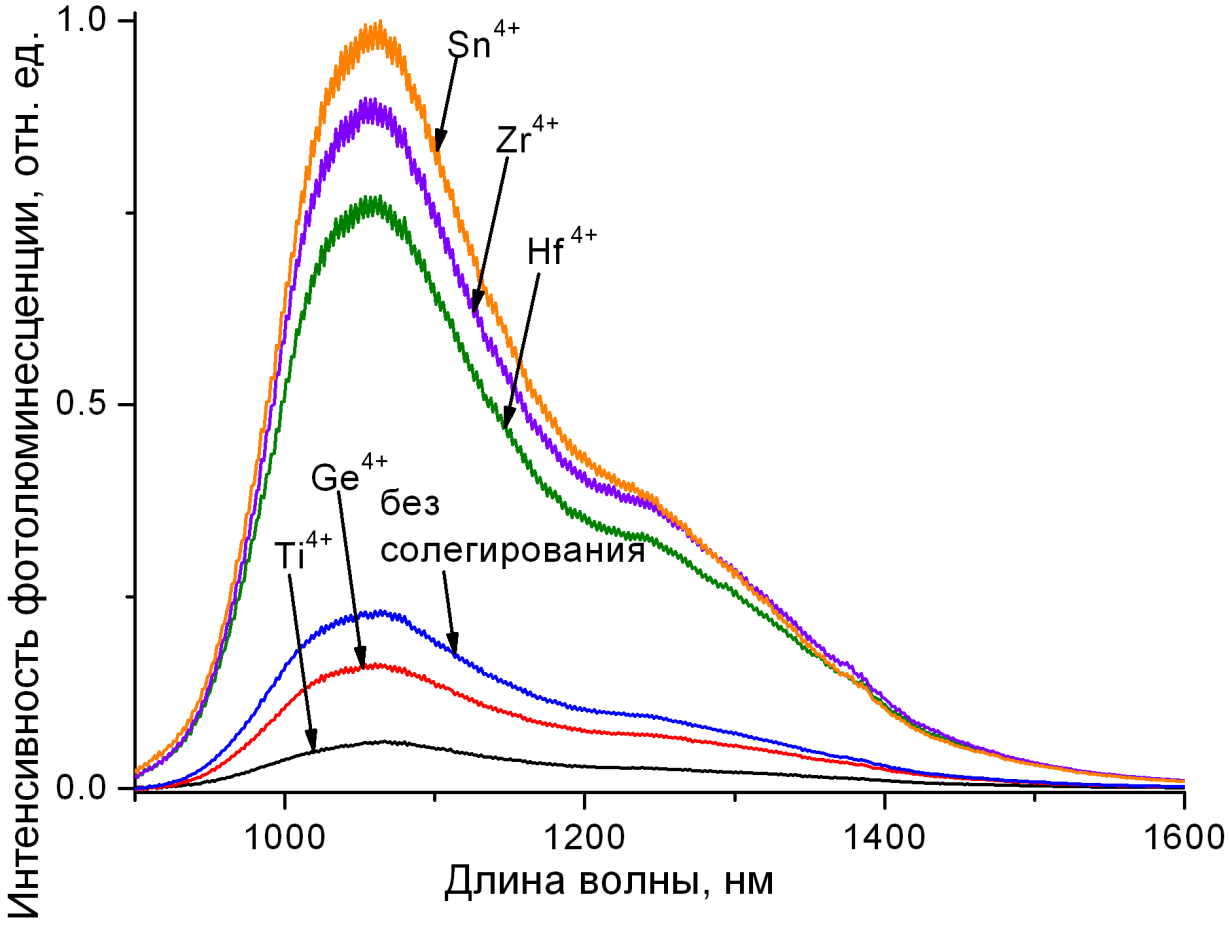
Интенсивность фотолюминесценции, отн. ед.
1.0
0.5
0.0
1000
1200
1400
1600
Длина волны, нм
Sn4+
Zr4+
Hf4+
Ge4+
Ti4+
без
солегирования

Fig. 3

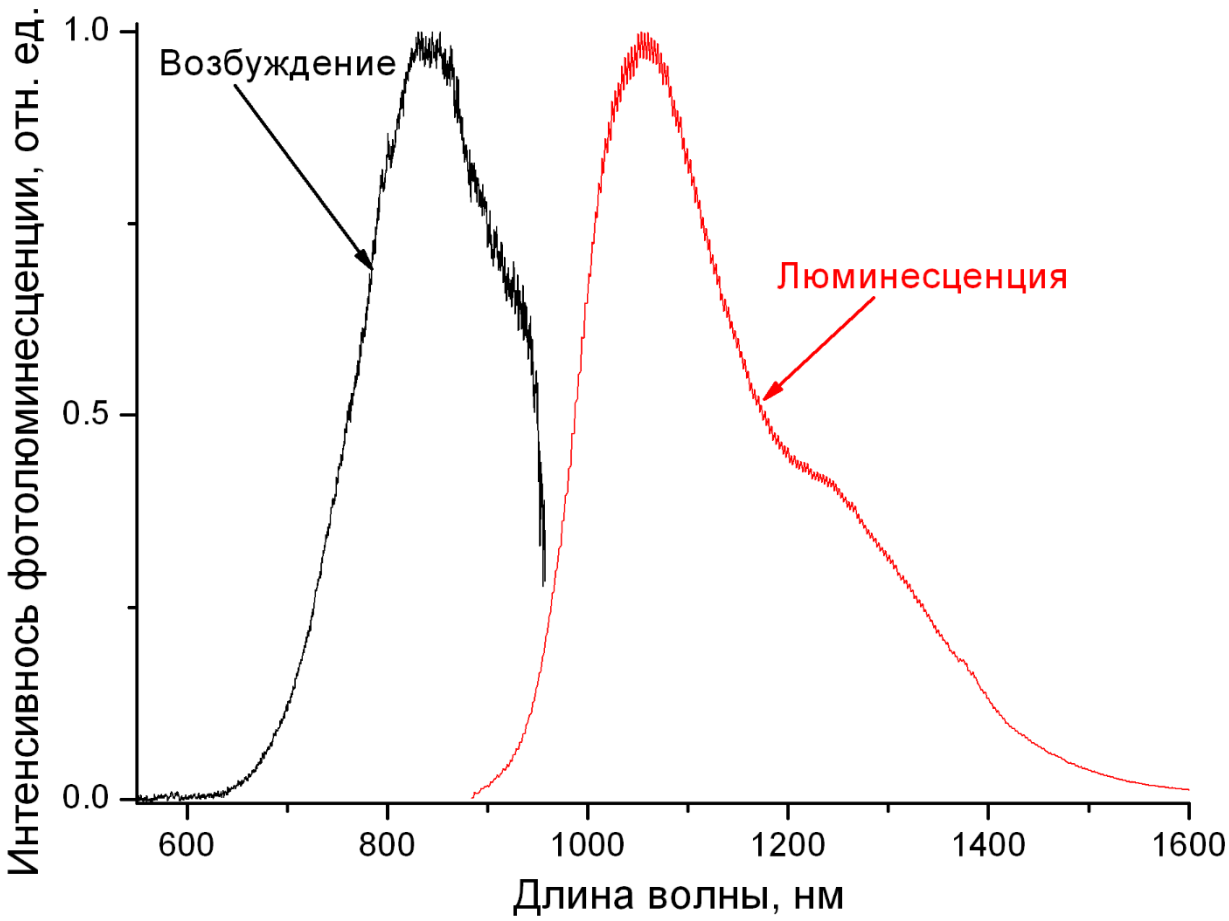
Интенсивнось фотолюминесценции, отн. ед.
1.0
0.5
0.0
Возбуждение
Люминесценция
600
800
1000
1200
1400
1600
Длина волны, нм

Fig. 4

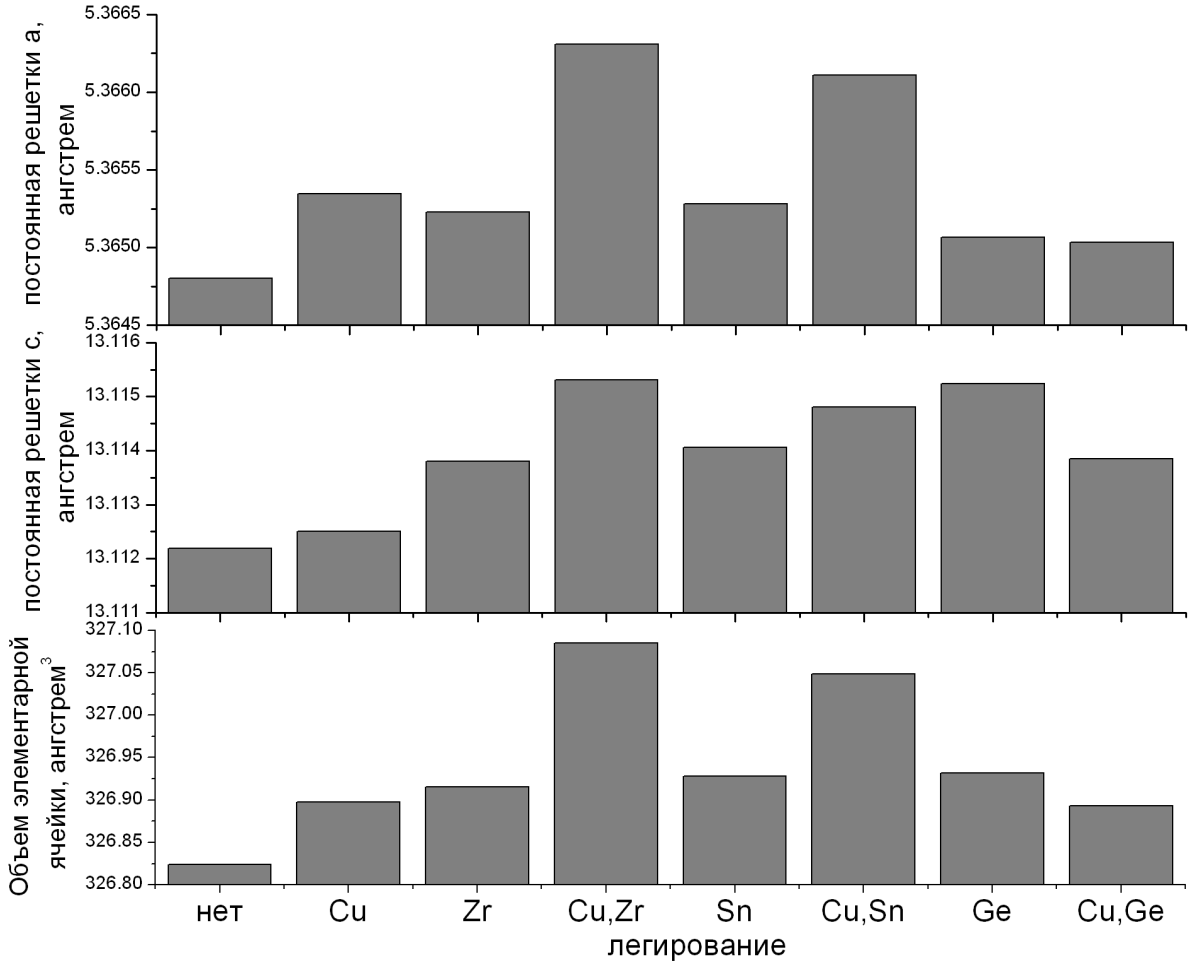
постоянная решетки a, ангстрем
5.3665
5.3660
5.3655
5.3650
5.3645
постоянная решетки c, ангстрем
13.116
13.115
13.114
13.113
13.112
13.111
Объем элементарной ячейки, ангстрем3
327.10
327.05
327.00
326.95
326.90
326.85
326.80
нет
Cu
Zr
Cu,Zr
Sn
Cu,Sn
Ge
Cu,Ge
легирование

Fig. 5